J Neurophysiol 106: 104–114, 2011.
First published April 13, 2011; doi:10.1152/jn.00896.2010.

Measurement of the extraocular spike potential during saccade countermanding

David C. Godlove, Anna K. Garr, Geoffrey F. Woodman, and Jeffrey D. Schall
Department of Psychology, Vanderbilt Vision Research Center, Center for Integrative and Cognitive Neuroscience, Vanderbilt Brain Institute, Vanderbilt University, Nashville, Tennessee

Submitted 18 October 2010; accepted in final form 11 April 2011

Godlove DC, Garr AK, Woodman GF, Schall JD. Measurement of the extraocular spike potential during saccade countermanding. *J Neurophysiol* 106: 104–114, 2011. First published April 13, 2011; doi:10.1152/jn.00896.2010.—The stop signal task is used to investigate motor inhibition. Several groups have reported partial electromyogram (EMG) activation when subjects successfully withhold manual responses and have used this finding to define the nature of response inhibition properties in the spinal motor system. It is unknown whether subthreshold EMG activation from extraocular muscles can be detected in the saccadic response version of the stop signal task. The saccadic spike potential provides a way to examine extraocular EMG activation associated with eye movements in electroencephalogram (EEG) recordings. We used several techniques to isolate extraocular EMG activation from anterior electrode locations of EEG recorded from macaque monkeys. Robust EMG activation was present when eye movements were made, but no activation was detected when saccades were deemed canceled. This work highlights a key difference between the spinal motor system and the saccade system.

electromyogram; stop signal task; inhibition; extraocular muscle; eye movement

RAPID INHIBITION of prepared motor responses has been studied extensively with the stop signal, or countermanding, task (for review, see Verbruggen and Logan 2008). In this task, subjects make quick responses to target stimuli. On a subset of trials, a second stimulus follows the target, instructing subjects to withhold their responses. When subjects are successful in canceling their responses, behavioral measures cannot be recorded because no overt behavior occurs. However, using a modeling approach, the timing of the covert inhibitory process can be estimated (Logan and Cowan 1984; Colonius 1990; Logan 1994). A saccadic response version of the stop signal task has been used to characterize properties of the ocular motor system (Hanes and Schall 1996; Hanes et al. 1998; Hanes and Carpenter 1999; Logan and Irwin 2000; Pare' and Hanes 2003; Corneil and Elsley 2005; Walton and Gandhi 2006; Boucher et al. 2007; Emeric et al. 2007).

Several groups have reported subthreshold electromyogram (EMG) activation on canceled trials in the manual response version of the countermanding task (De Jong et al. 1990; McGarry and Franks 1997; McGarry et al. 2000; van Boxtel et al. 2001; Scangos and Stuphorn 2010). However, it is unknown if partial extraocular EMG activation is present when eye movements are deemed canceled. The possibility that extraocular muscles may contract without producing detectable eye movement seems unlikely. However, the literature is inconclusive on this point. While it is true that the inertia of the eye within the orbit is negligible, the surrounding tissue of the oculomotor plant exerts viscous and elastic forces on the eye that are significant (Porter et al. 2003). It is difficult to estimate the extent to which these forces counteract eye movement production, because research has resulted in contradictory evidence (Robinson 1964; Sklavos et al. 2005; Anderson et al. 2009; Quaia et al. 2009). In fact, very few experiments have been reported on this matter. Furthermore, most of these studies have been conducted using anesthetized animals, but larger time constants for viscoelastic relaxation of orbital tissues have been noted in alert animals (Anderson et al. 2009).When considering whether or not extraocular muscles are able to generate contractions that do not result in eye movements, it is also important to consider the muscles themselves. The extraocular muscles are relatively poor actuators. During periods of fixation, only 23% of muscle innervation is ultimately transferred to the tendons to result in rotation of the eyeball (Quaia and Optican 2003). Thus, when saccades are initiated, a force of much larger magnitude must be supplied to overcome that dissipated by the muscles themselves. This initial burst of force can be observed in the well-known "pulse-slide-step" discharge pattern of oculomotor neurons (Fuchs and Luschei 1970; Robinson 1970). The "pulse" portion of muscle innervation is thought to be necessary to overcome static viscous drag exerted by the passive orbital tissue (Sparks 2002). These considerations leave open the possibility that small extraocular muscle contractions may occur in the absence of detectable eye movements.

If partial EMG activation was observed in the primate ocular motor system when trials were deemed canceled, it would provide a powerful and versatile tool for examining motor control in saccadic tasks. This development would be particularly useful for neurophysiological research, since most of the work using the stop signal paradigm with monkeys has been carried out in the ocular motor domain. On the other hand, there is reason to believe that partial muscle activation should not be readily produced by the primate ocular motor system. First, saccades are thought to be initiated in an all-or-none manner. Second, although manual responses can be canceled by coactivating agonist and antagonist muscles, it should be nearly impossible to perform this type of cancelation in the ocular motor domain. The contralateral inhibitory circuitry of the brain stem saccade generator precludes this type of muscle coactivation (Hikosaka et al. 1978; Sparks 2002; for review, see Scudder et al. 2002).

Because of their positions in the orbit, it is difficult to record EMGs directly from the extraocular muscles. However, an

Address for reprint requests and other correspondence: J. D. Schall, PMB 407817, 2301 Vanderbilt Place, Vanderbilt Univ., Nashville, TN 37240-7817 (e-mail: jeffrey.d.schall@vanderbilt.edu).

 0022-3077/11 Copyright © 2011 the American Physiological Society

Downloaded from jn.physiology.org on December 9, 2011

electroencephalographic (EEG) effect associated with eye movements, the saccadic spike potential (SP), has been consistently noted in humans and monkeys (Blinn 1955; Keren et al. 2010; Sander et al. 2010). Several studies have provided strong evidence that the SP does not originate in cortical activity or from the corneoretinal potential (Thickbroom and Mastaglia 1985; Moster and Goldberg 1990; Picton et al. 2000). Instead, this component is myogenic, derived from contraction of the lateral and medial recti (Blinn 1955; Thickbroom and Mastaglia 1985). The SP appears as a prominent, high-frequency component occurring just before or concomitant with saccade onset. It takes the form of a frontal negativity with scalp distribution ipsilateral to the direction of eye movements (Thickbroom and Mastaglia 1985; Moster and Goldberg 1990; Keren et al. 2010). With appropriate filtering techniques, SPs have been shown to reliably precede saccades as small as 0.2° in amplitude and to predict saccades with amplitudes of <0.2° above chance level (Keren et al. 2010).[1] Research on the SP has lapsed over the last few decades, but interest was recently renewed with the observation that many findings of γ-band activity in scalp EEG recordings that were attributed to cognitive processes may actually have been artifacts from the SP associated with microsaccades (Yuval-Greenberg et al. 2008). Consequently, methods for isolating and removing SP activation from EEG recordings have been described (Keren et al. 2010).

In the present study, we tested the hypothesis that partial activation of eye movement responses are made in the stop signal task, similar to findings from manual stop signal studies. This hypothesis predicts that partial muscle activation can occur on canceled trials. We tested this prediction by recording EEG and isolating SPs during periods when eye movements were prepared but not detected. We found strong SPs when saccades were made but found no evidence of SP activation when movements were deemed canceled.

METHODS

Animal care. Data were collected from one male bonnet macaque monkey (*Macaca radiata*; ~8.5 kg) and one female rhesus macaque monkey (*Macaca mulatta*; ~7 kg). Both animals were cared for in accordance with policies set forth by the United States Department of Agriculture and Public Health Service Policies on the Humane Care and Use of Laboratory Animals. Animal care, procedures, and experiments were also carried out with supervision and approval from the Vanderbilt Institutional Animal Use and Care Committee. Fruit juice was given as positive reinforcement for correctly completed trials. During periods of testing, ad libitum access to liquids was withdrawn. In consultation with attending veterinarians, each animal's weight and food intake were monitored, and fluids were supplemented as needed.

Surgical procedures. All surgical procedures were carried out under aseptic conditions. Access to food was withdrawn 12 h before surgery. Animals were sedated with ketamine (10–30 mg/kg) and provided with an initial dose of buprenorphine (0.005–0.010 mg/kg) to alleviate postoperative discomfort. Ophthalmic ointment was applied to prevent corneal drying. Robinul (0.004–0.008 mg/kg) was administered to minimize mucosal secretions and help prevent vagal bradycardia. Animals were intubated, and catheters were inserted into the saphenous veins for the administration of support fluids throughout the procedure. Monkeys were anesthetized with an isoflurane-oxygen mixture (1–3% $C_3H_2ClF_5O$), shaved, positioned in stereotax, and scrubbed. ECG, rectal temperature, respiration, and blood pressure were monitored. Expiratory CO_2 was maintained at ~4%. After the subcutaneous administration of lidocaine (~1–2 ml of 2% solution), the subjects' skulls were exposed, and titanium headposts were firmly attached with titanium orthopedic screws (Synthes, West Chester, PA) to immobilize the animals' heads during testing. Solid gold surface electrodes, Teflon-coated stainless steel wires, and plastic connectors were constructed and implanted following the method of Woodman et al. (2007). Surgical sutures and staples were used to close incisions in layers. In consultation with attending veterinarians, analgesics [bupronorphine (0.005–0.010 mg/kg)] and prophylactic antibiotics [naxcel (2.2 mg/kg)] were administered for at least 3 days after surgery.

Task. During testing, monkeys were seated comfortably 51 cm from a cathode ray tube monitor (48 × 48°, 80 Hz) in enclosed polycarbonate and stainless steel primate chairs and head restrained using surgically implanted headposts. Stimulus presentation, task contingencies related to eye position, and delivery of liquid reinforcement were all under computer control in hard real time (TEMPO, Reflective Computing, Olympia, WA). Stimuli were presented using computer-controlled raster graphics (TEMPO Videosync 1,280 × 1,040-pixel resolution, Reflective Computing). Stimuli had a luminance of 30 cd/m^2 (fixation point) or 10 cd/m^2 (targets) on a 1-cd/m^2 background.

Behavior and electrophysiological signals were recorded during the countermanding (i.e., stop signal) task (Fig. 1). Additional details about the behavioral training regime and task have been previously described (Hanes and Schall 1995; Hanes et al. 1998). Trials were initiated when monkeys fixated a centrally presented square, which subtended 0.34° of the visual angle. After a foreperiod ranging from 200 to 1,100 ms, the central fixation point was extinguished, and a target subtending 3° of the visual angle simultaneously appeared at 10° to the left or right of fixation. The foreperiod was randomly sampled from a distribution described by the following function:

$$p(t) = [1 - \exp(-t/\tau_g)] \times [\exp(-t/\tau_d)]$$

where $p(t)$ is the probability of selecting a specific foreperiod, t is time, τ_g is the growth rate, and τ_d is the decay rate. We chose a growth rate of 1,000 ms and a decay rate of 200 ms to approximate a nonaging foreperiod. We added 200 ms to this distribution and truncated it at 1,100 ms to achieve the desired range. On no-stop trials (Fig. 1, *top*), no further visual stimuli were presented. Monkeys were required to make a saccade to the target within 600 ms to obtain a reward. Correct trials were rewarded with several drops of juice and an audible tone. On stop trials (Fig. 1, *bottom*), the fixation point was reilluminated after a variable delay, providing a "stop signal" that instructed the monkeys to cancel their impending eye movements and maintain central fixation. In practice, two trial outcomes were then possible. If monkeys successfully withheld the eye movement and maintained fixation for a minimum of 600 ms, they obtained a juice reward and a tone. These trials were designated as "canceled." If monkeys were unable to inhibit the movement, a 1,500-ms timeout was added to the normal intertrial interval of 200 ms, no rewards were given, and the trial was termed "noncanceled." The stop signal delay (SSD), or time between the target and stop signal presentation, determines the probability with which movements can be successfully countermanded (Logan and Cowan 1984). An initial set of SSDs from 0 to 420 ms and separated by either 40 or 60 ms was selected for each recording

[1] Keren et al. (2010) reported data from a bin that included saccade amplitudes ranging from 0.2 to 0.5°. As correctly pointed out by an anonymous reviewer, the distribution of saccade amplitudes within this bin was not reported. Strictly speaking, it is therefore impossible to say with certainty that SPs associated with saccades of 0.2° in amplitude could be reliably detected. However, it is well known that histograms displaying amplitudes of saccades recorded during a given time interval tend to take the form of decreasing exponential distributions (e.g., Collewijn and Kowler 2008). In other words, for any given distribution, saccades of smaller amplitude tend to be made with exponentially higher frequency than saccades of larger amplitude. Therefore, it is reasonable to expect that saccades with amplitudes of ~2° made up a large proportion of the saccades used for this analysis.

Downloaded from jn.physiology.org on December 9, 2011

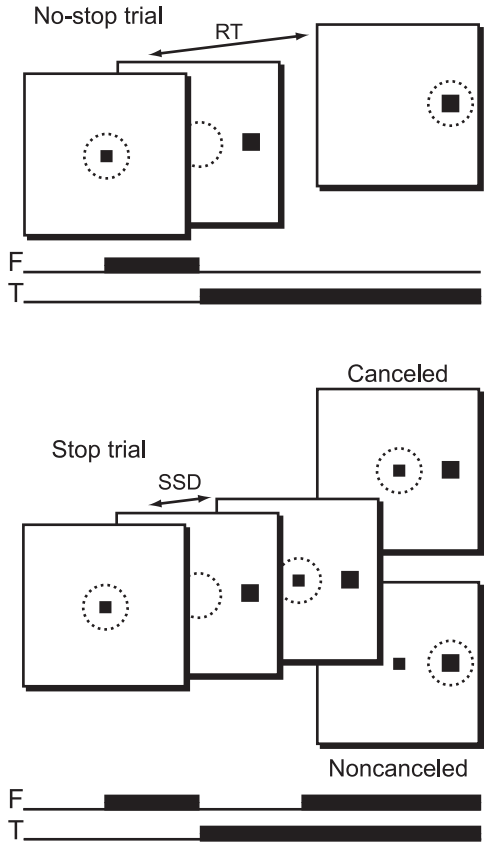

Fig. 1. The stop signal (or countermanding) task in a schematic representation. No-stop trials (*top*) were initiated when monkeys fixated a centrally presented fixation point. After a variable time, the fixation point was extinguished and simultaneously a peripheral target was presented at one of two possible locations. Monkeys were required to fixate targets with quick saccades for juice rewards. Stop trials (*bottom*) were initiated in the same way. After a variable time, termed the stop signal delay (SSD), the fixation point was reilluminated, instructing the monkeys to withhold movement. Successful inhibition of saccades resulted in a reward (canceled trials), but errant saccades resulted in no reward (noncanceled trials). The solid squares indicate stimulus locations. Dotted circles represent the area of fixation. F, fixation point; T, target; RT, reaction time.

session. We then manipulated the SSD using an adaptive staircasing algorithm, which adjusted the stopping difficulty based on performance. When subjects failed to inhibit responses, the SSD was decreased by a random step of 1, 2, or 3, increasing the likelihood of success on the next stop trial. Similarly, when subjects were successful in inhibiting the eye movement, the next SSD was increased by a random step of 1, 2, or 3, decreasing the future probability of success. This procedure was used to ensure that subjects failed to inhibit action on ~50% of stop trials overall. Stop trials were 30–70% of all trials in a given session, with a typical session consisting of several thousand trials. Reaction time (RT) data did not show any evidence that subjects slowed responses to "wait for" the stop signal (see RESULTS). Saccade initiation and termination were detected offline using a custom algorithm implemented in the MATLAB programming environment (MathWorks, Natick, MA), which first detected instantaneous velocity elevated above 30°/s and then calculated the beginning and ending of the monotonic change in eye position.

Data acquisition. Time stamps of relevant trial events were recorded at 1 kHz with analog data using a Plexon Multichannel Acquisition Processor (MAP) box (Plexon, Dallas, TX). Eye position was monitored using a video-based infrared eye tracking system (ASL, Bedford, MA) and was streamed to the Plexon MAP box parallel with trial events and EEG data using a 64-channel Plexon Breakout Board. We estimated the spatial resolution of our eye tracking setup by recording SDs while monkeys were actively fixating the central fixation point. Across all sessions, the mean SDs were ±0.54° and ±0.51° for *monkeys F* and *Y*, respectively. The maximum SDs while fixating for a session were ±0.74° and ±0.67° for *monkeys F* and *Y*, respectively. Unfortunately, this spatial resolution was not high enough to detect microsaccades, although it was more than sufficient to detect the onsets of large task-related responses. Implanted EEG surface electrodes were referenced to clip-style Ag/AgCl cup electrodes (Electro-Cap, Eaton, OH), which were filled with conductive paste and clipped to either the left ear (*monkey F*) or linked to both ears (*monkey Y*). All data were recorded from an electrode approximating Fz of the international 10–20 system for humans in *monkey F* and an electrode approximating Fpz in *monkey Y*. Since data were reported from a single midline electrode in both subjects, the asymmetric referencing used for *monkey F* did not result in any significant differences. The EEG from each electrode was amplified with a high-input impedance head stage (>1 GΩ , ~2 pF of parallel input capacitance, HST/8o50-G1-GR, Plexon) and filtered between 0.7 and 170 Hz with two cascaded, one-pole, low-cut, Butterworth filters and a four-pole, high-cut, Butterworth filter.

Race model behavioral analysis. The race model has been used with great success to account for both behavioral performance and neural activity in the countermanding paradigm (Logan and Cowan 1984; Boucher et al. 2007; Lo et al. 2009; for a review, see Verbruggen and Logan 2008). On no-stop trials, RTs can be observed directly. On stop signal trials, noncanceled RTs can be recorded, along with the probability of committing an errant noncanceled saccade at each SSD. The latter measure tends to assume the form of an increasing sigmoid curve and has traditionally been referred to as an inhibition function. By treating the inhibition function as a cumulative probability distribution and comparing it with the distribution of RTs on no-stop trials, one is able to use the logic of the race model to estimate the median time required to cancel the execution of a motor response (Logan 1994; Band et al. 2003; see also Colonius 1990). This stop signal RT (SSRT) provides a measure of the otherwise covert stop process.

Following the methods of Hanes et al. (1998), we first fitted a Weibull function [$W(t)$] with the following form to the inhibition function for each monkey averaged across sessions:

$$W(t) = \gamma - (\gamma - \delta) \times \exp[-(t/\alpha)^{\beta}]$$

where γ is the maximum probability value, δ is the minimum probability value, t is the time after target onset, α is 64% of the maximum probability value, and β is the slope. Next, we used the fitted inhibition functions and the combined no-stop RT data to estimate SSRTs for each monkey using two different methods. The first of these methods assumed that SSRT was a random variable, whereas the second method assumed that SSRT was constant across SSDs (Hanes et al. 1998; Band et al. 2003). Since there was no reason to suppose an advantage of either of these SSRT estimation methods, we averaged the two estimates together to obtain a final SSRT estimate separately for each monkey (Hanes et al. 1998; Pare' and Hanes 2003).

A robust finding in the stop signal literature is that noncanceled RTs are significantly lower than no-stop RTs. This is a straightforward prediction of Logan and Cowan's (1984) horse race model, since trials with faster "go" processes will tend to finish before the "stop" process, thus escaping behavioral inhibition. It also suggests that noncanceled trials cannot be accurately compared with the entire distribution of no-stop trials when RT is a potential confounding variable. An accurate comparison can only be made between noncanceled trials and no-stop trials with relatively faster RTs. Specifically, noncanceled trials should only be compared with no-stop trials with RTs < SSRT + SSD. These are the trials that would have escaped behavioral inhibition and resulted in errant saccades had a stop signal been presented. Similarly, for accurate comparisons, canceled trials must be matched to slower no-stop trials with RTs > SSRT + SSD. Thus, even though

Downloaded from jn.physiology.org on December 9, 2011

no response is generated on successfully canceled trials, RT ranges can be estimated for this trial type. The technique of matching noncanceled and canceled trials to no-stop trials with RTs from the appropriate portion of the RT distribution has been termed "latency matching" (Hanes et al. 1998). In the present study, it was especially important that we compared canceled trials with their latency-matched no-stop counterparts. This allowed us to estimate times when eye movements were likely even though they were not detected. Where appropriate, we used our derived SSRT estimates to latency match at each SSD.

Event-related potential and event-related velocity analyses. Event-related potentials (ERPs) were time locked to saccade initiation or target onset and baseline corrected to the interval from 150 to 50 ms before these events. Canceled trials did not contain saccade events. Instead, a virtual saccade event was created for trials in this condition by randomly sampling from the distribution of latency matched no-stop RTs with replacement. Canceled trials were then aligned to this virtual saccade event and baseline corrected. Trials with voltage deflections greater than ± 300 μV due to artifacts were excluded from further analysis. This threshold for rejection was an order of magnitude greater than the variability in the ERPs observed across monkeys (i.e., maximum root mean square for *monkey F* target-aligned no-stop trials: 42.2 μV, canceled trials: 39.8 μV, noncanceled trials: 41.4 μV; and maximum root mean square for *monkey Y* target-aligned no-stop trials: 42.7 μV, canceled trials: 45.2 μV, and noncanceled trials: 40.7). Single trial EEG signals were truncated 50 ms before the onset of the second, nontask-related saccade to eliminate "smeared" saccade-related artifacts. It was important to estimate the relative timing of saccades and to display this estimate graphically. Instead of using a traditional method such as displaying a histogram of saccade latencies, we collapsed across saccade velocity profiles. This method is essentially the same as creating an ERP from EEG data except that the data were radial eye velocity traces (Fig. 2). The resulting average not only contained information about saccade latency but also took into consideration saccade amplitude and duration, making it a more complete descriptor of average saccade dynamics. Since these velocity profiles were aligned to particular events and collapsed across trials in the same way as ERPs, we will refer to them as "event-related velocities" (ERVs). ERVs were not baselined since an ERV value of zero is not arbitrary as it is in an ERP. As a rule, the single trial velocity profiles that made up the ERVs were truncated at the onset of the second, nontask-related saccade to avoid contamination of the task-related saccade velocity trace.

Narrow digital bandpass filters (frequency: ± 1 Hz) were used to discriminate the SP from other saccade-related components (see RESULTS). Each filter was created using a Hamming window of length $(2 \times T + 0.001)$ s, where $T = 1/f$. A zero phase-shift digital filter was applied to the data using the specified Hamming window. The analytic power of the filtered data at each time interval (t_i) was approximated using a sliding window function of the following form:

$$P(t_i) = \frac{\max(A) - \min(A)}{2}$$

where A is the time interval $[t_i - (T/2) \times t_i + (T/2)]$. These methods ensured a high level of filter specificity while minimizing sacrifices in timing estimation accuracy at each bandpass frequency.

A signal-to-noise ratio was estimated for each applied filter to assess how well it isolated the SP from the surrounding EEG. After each filter was applied to a single session of data and analytic power was estimated, the mean value in a 41-ms time window centered on the peak of the SP was recorded. This value was termed the "signal." The mean value in a 1-s time window centered on the saccade onset and excluding the signal time window was also recorded. This value was termed "noise." (Note that in this context, noise does not just refer to variability, measurement error, or unwanted line voltage fluctuations; noise also refers to EEG fluctuations and includes those fluctuations that are task related. Task-related EEG fluctuations do not average out in ERPs, and they can obscure the SP, which is our component of interest.) The filter yielding the highest signal-to-noise ratio was then used to isolate single trial SPs in subsequent analysis.

RESULTS

Behavior. RTs, average probabilities of committing errors, and SSRT estimates collapsed across sessions are shown in Table 1. Both animals exhibited noncanceled trials with probability $> 50\%$. Since we used a staircasing algorithm to adjust SSD, this departure suggests that both animals tended to speed up, causing a reduction in SSD. This pattern of behavior has been described before in animals performing the saccade stop signal task, and it appears to be an effective strategy for speeding up trial presentation and maximizing the rate of reward delivery (Godlove et al. 2009). In any case, our estimates of SSRT were lower than the more typical estimates of

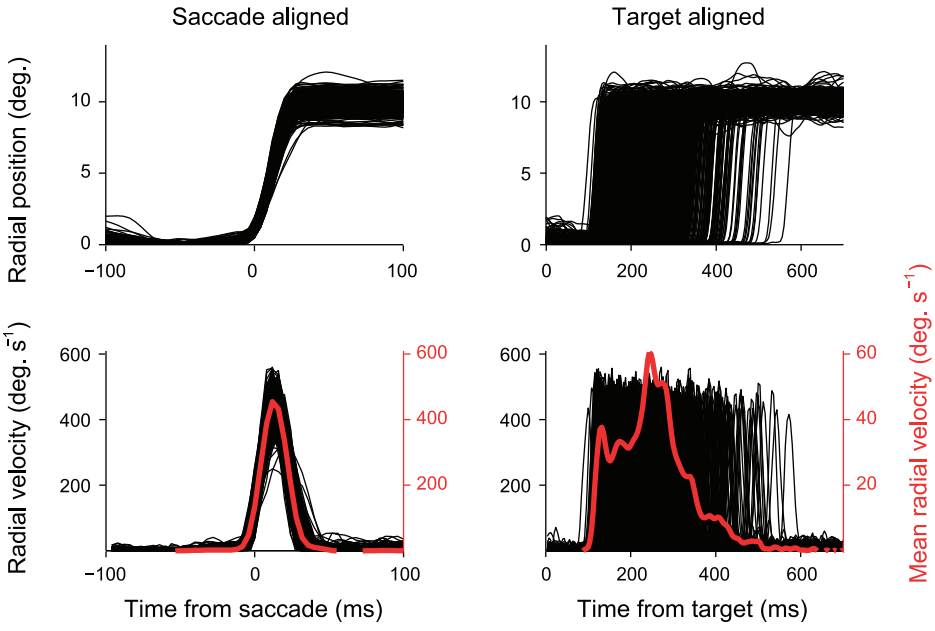

Fig. 2. The timing of eye movements relative to task events was displayed using event-related velocity (ERV) plots. This technique is similar to creating event-related potentials (ERPs) from raw electroencephalogram (EEG) signals. *Top left*: single trial radial positions for a sample session aligned on the saccade onset. *Bottom left*: instantaneous radial velocity for the same trials (black) along with the mean instantaneous velocity collapsed across all trials (red). *Top right*: same single trial radial positions in relation to the target onset. *Bottom right*: single trial instantaneous velocity in relation to the target onset as well as the average radial velocity collapsed across all trials. This target-aligned ERV gives information about the average saccade latency, velocity, and duration relative to the target onset.

Downloaded from jn.physiology.org on December 9, 2011

Table 1. *Summary statistics for stop signal task performance*

	No-Stop RT	Noncanceled RT	*P* (Noncanceled)	SSRT
Monkey F	224 ± 52	211 ± 57	0.58	59
Monkey Y	243 ± 77	206 ± 75	0.53	59

Values are means ± SD. Shown are reaction times (RTs), probabilities of committing errant noncanceled saccades (*P*), and stop signal RTs (SSRTs) for each subject collapsed across sessions.

80–100 ms recorded in the literature. If our estimates were artificially low due to violations of the race model, it presents a problem for latency matching, since we may have erroneously underestimated the time of probable SP activation on canceled trials. Accordingly, when the results depended on latency matching, large RT windows were displayed and analyzed to ensure that late SP activation was not missed in canceled trials.

Saccade dynamics. Figure 3 shows main sequences of no-stop (blue) and noncanceled (red) saccades separately for each subject and each target. These data are shown numerically in Table 2. We carried out three-way ANOVAs to test the hypotheses that saccade amplitude and/or velocity differed between subjects, targets, or trial types. Both amplitude [$P < 0.001$, degrees of freedom (df) = 87] and velocity ($P < 0.001$, df = 87) were found to differ between targets. Monkeys tended to make slightly larger amplitude and higher velocity saccades toward the right target. This may be an artifact induced by the monocular eye tracking procedures we used. Since we only tracked the right eye of each subject, saccades traces to the right target reflected abduction of the tracked eye, whereas saccade traces to the left target reflected adduction of the tracked eye. On the other hand, the difference may reflect a real bias that both monkeys developed toward the right target. Peak saccade velocity was also found to differ between subjects ($P < 0.001$, df = 87). *Monkey F* made saccades with higher peak velocities than *monkey Y*. However, neither amplitude ($P = 0.701$, df = 87) nor peak velocity ($P = 0.380$, df = 87) differed significantly between trial types. Since main effects of ~1° proved highly significant in the target contrast, the failures to reject null hypotheses in the trial type contrasts cannot be attributed to a deficiency of statistical power. These results replicate previous findings by Hanes and Schall (1995).

Saccade-aligned ERPs. Figure 4 shows saccade-aligned ERPs and ERVs from both subjects. On trials in which saccades were detected, we observed a high-amplitude, high-frequency negativity occurring concomitant with or slightly before saccade initiation. This saccade-related component has been described many times in human subjects (Evdokimidis et al. 1991; Everling et al. 1997) and at least once in nonhuman primates (Sander et al. 2010).

For our purposes, the most important finding was the absence of the SP on canceled trials. At least two alternatives exist to explain this finding. First, we may conclude that partial muscle activation does not occur on canceled saccade trials, so no saccadic SP is evident. Second, we may conclude that aligning EEG to a virtual saccade event obtained by random sampling from existing RT distributions is too coarse a method to detect the saccadic SP on canceled trials. If partial motor activation did occur on these trials, we do not know when. Therefore, aligning on virtual randomly sampled RT events and collapsing across the data may have smeared any partial SPs and rendered them difficult to detect. We note that even if small-amplitude SPs had been generated on the canceled trials but were temporally smeared by averaging, they should be revealed by a low-amplitude, broad negativity during the measurement epoch. As is evident in Fig. 4, we did not observe a waveform on canceled trials, consistent with this pattern. However, we carried out an additional time-frequency analysis

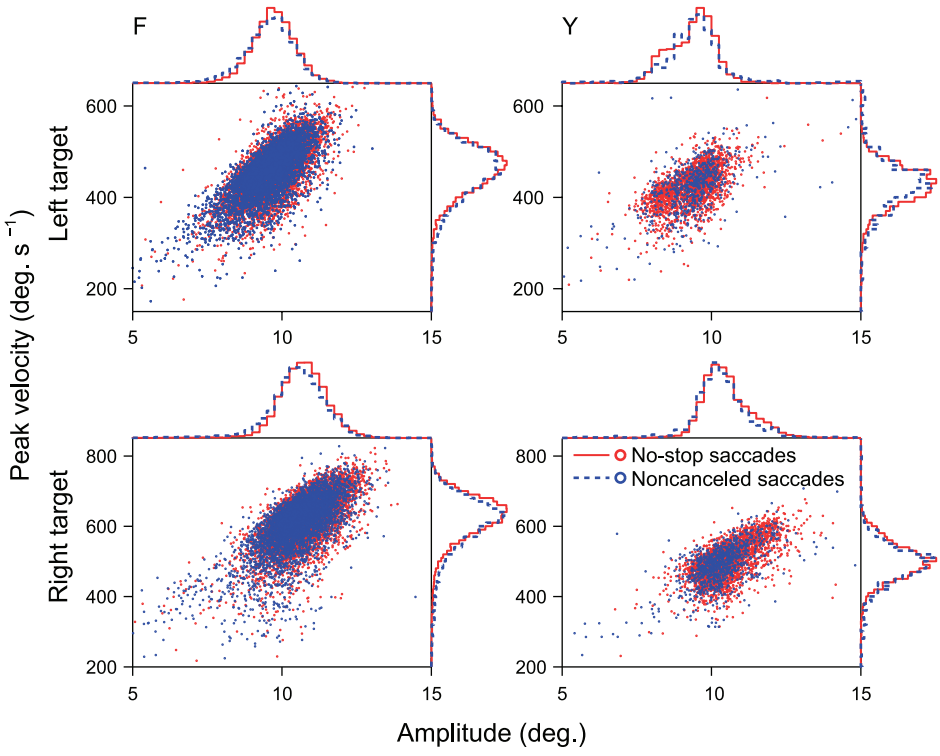

Fig. 3. Saccade dynamics do not differ between no-stop and noncanceled trials. The scatterplots show saccade amplitude versus peak saccade velocity (main sequences) across all sessions. The histograms display associated probability densities for each measurement. Bin widths are 10°/s for velocity distributions and 0.25° for amplitude distributions. Blue dots and dashed lines represent saccades on no-stop trials. Red dots and solid lines represent saccades on noncanceled trials. Rows separate data by target; columns separate data by subject.

Downloaded from jn.physiology.org on December 9, 2011

Table 2. *Countermanding saccade dynamics*

	Amplitude, °				Peak Velocity, °/s			
	Left target		Right target		Left target		Right target	
	No stop	Noncanceled	No stop	Noncanceled	No stop	Noncanceled	No stop	Noncanceled
Monkey F	9.7 ± 0.7	9.6 ± 0.9	10.7 ± 0.8	10.5 ± 1.2	473 ± 92	463 ± 97	623 ± 66	607 ± 104
Monkey Y	9.3 ± 0.9	9.8 ± 2.9	10.5 ± 0.9	10.5 ± 2.2	428 ± 97	469 ± 306	502 ± 52	509 ± 247

Values are means ± SD. Shown are mean amplitudes and mean peak velocities across sessions separated by subject, target location, and trial type.

to isolate SP activation from the surrounding EEG and test for the presence of extraocular EMG activation during canceled stop trials.

Isolated SP activation. In our data, the SP is readily visible as a stereotyped high-frequency negativity (Fig. 4). Because of its unusually high frequency and its invariance across sessions, we hypothesized that SP activation could be discriminated from the surrounding EEG on a trial-by-trial basis after the application of an appropriate filter (see also Keren et al. 2010). We applied narrow digital bandpass filters in steps of 10 Hz to search for a frequency that optimally discriminated SP activation from the surrounding EEG. After filtering the data and calculating power as a function of time, we constructed response-aligned ERPs for no-stop trials at each bandpass frequency for each recording session. We then calculated signal-to-noise ratios for each filtered ERP. The result of this analysis is shown in Fig. 5*F*. A bandpass filter centered on 95 Hz was found to provide the greatest discrimination between the SP and the surrounding EEG for *monkey F*, whereas a bandpass filter centered on 35 Hz was found to be optimal for *monkey Y*. At first glance, this difference may seem surprising. However, our technique does not simply measure the frequencies contributing power to the SP. Instead, it isolates the frequency that optimally discriminates the SP from the surrounding EEG. Therefore, this difference reflects variations in overall EEG frequency spectra between the two monkeys. Differences in EEG frequency spectra are to be expected due to several factors. For example, the skulls of *monkeys F* and *Y* were observed to be of different thicknesses during surgery (Nunez and Srinivasan 2006).

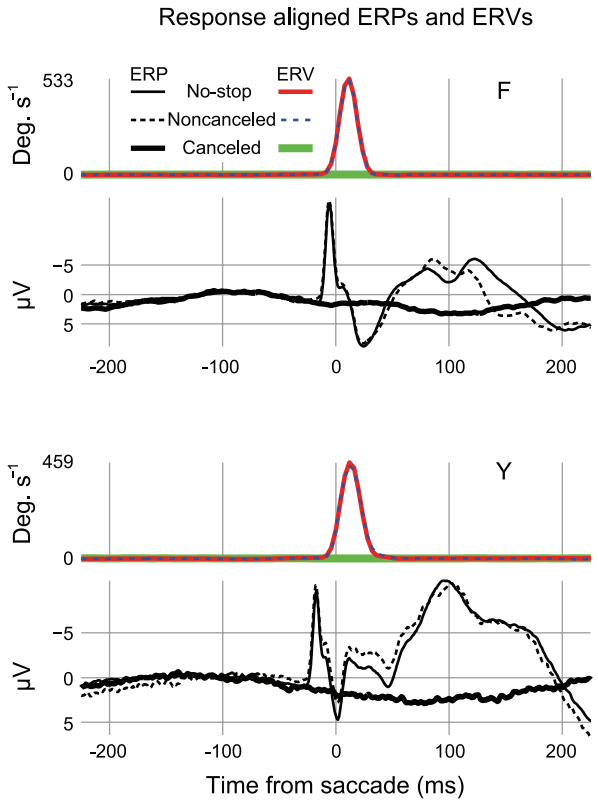

Fig. 4. No saccadic spike potentials (SPs) are evident in canceled trials aligned on a virtual saccade event. Black traces show ERPs and colored traces show ERVs (see text). The thin solid traces show saccade-aligned ERPs and ERVs on no-stop trials. The most prominent components in the ERPs are the sharp negative SPs, which occur just before or concomitant with the saccade onset and the several positive and negative deflections that follow. The first several components that follow the saccade onset probably include a strong contribution from the corneoretinal potential. The dashed traces show ERPs and ERVs on errant noncanceled trials. Note the extreme similarity of the ERVs for no-stop and noncanceled trials. Also note the similarity between no-stop and noncanceled ERPs. This similarity is especially apparent in the time before the saccade onset when the SP is visible. The thick solid traces show ERPs and ERVs on canceled trials aligned to a virtual saccade event. No elevated velocity can be detected in the ERVs, and no SP can be detected around *time 0* in the ERP. Data were collapsed across 15 sessions and recorded from a location approximating Fz for *monkey F*; data were collapsed across 7 sessions and recorded from a location approximating Fpz for *monkey Y*. ERP data were baselined to the period from 150 to 50 ms before the saccade onset. The numbers of trials (n) in each ERP were as follows: *monkey F*, no-stop n = 13,764, canceled n = 6,256, and noncanceled n = 6,552; and *monkey Y*, no-stop n = 4,782, canceled n = 1,489, and noncanceled n = 1,120.

The application of optimal discrimination bandpass filters allowed us to observe the SP separate from the surrounding EEG. Using this technique, we were able to search for SP activation in target-aligned ERPs made up either of no-stop or canceled trials. This comparison is shown for a sample session from *monkey F* in Fig. 6. The SP was visible in the unfiltered data when aligned on the response onset but was impossible to resolve, even on no-stop trials, when aligned on the target onset (*left* column). After filtering, the SP was readily apparent in the response-aligned, single trial data as a vertical band of elevated power (Fig. 6, *top right*). A diffuse band of power can also be observed in the target-aligned no-stop trials during the period of time when saccades were initiated (Fig. 6, *middle right*). However, no coherent band of elevated power could be discriminated on successfully canceled trials (Fig. 6, *bottom right*).

Our bandpass filtering technique also provided us with power measurements that were amenable to statistical testing. After filtering the data and performing latency matching to compare canceled trials with the appropriate no-stop trials, we measured average normalized power during a discrete window around mean RTs. For our window, we chose the period from the 25th percentile RT to the 75th percentile RT. Following this method ensured that we sampled power on canceled trials during the period of time when SPs were most likely to occur.

Downloaded from jn.physiology.org on December 9, 2011

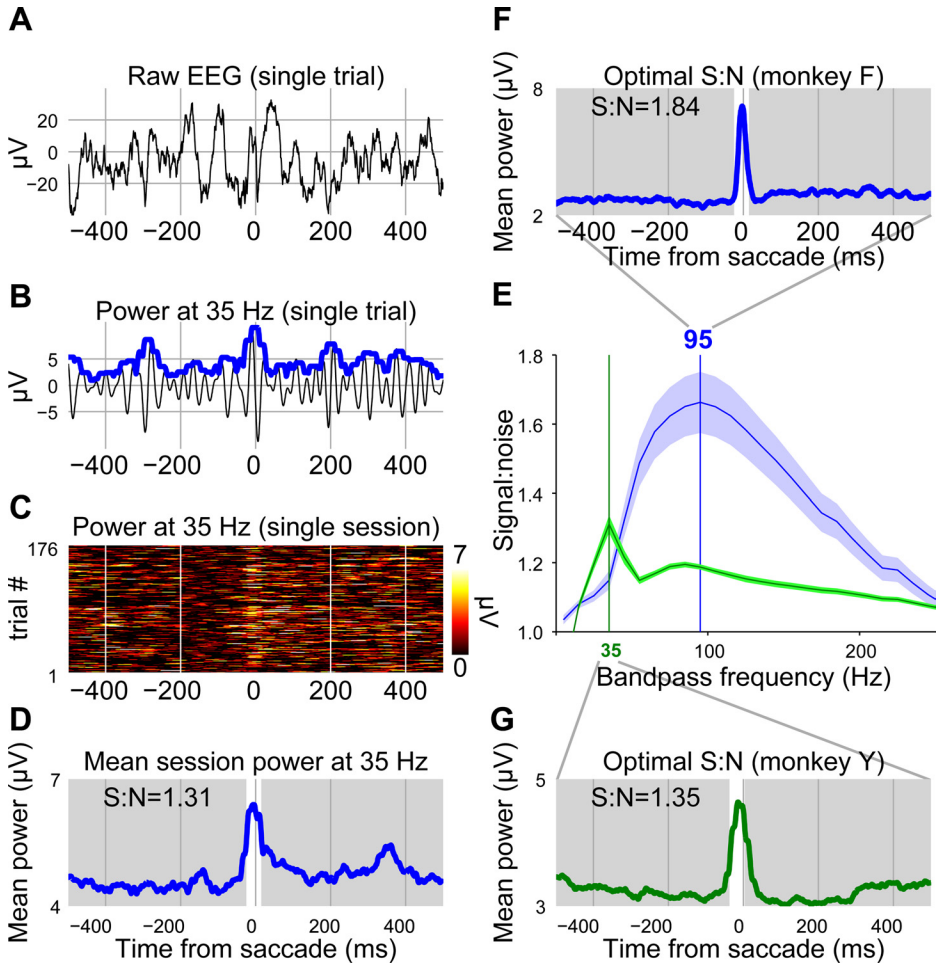

Fig. 5. Bandpass filters were optimized to find frequencies that allowed for the highest discrimination between the SP and non-SP components. *A*: 1-s example of raw EEG centered on the saccade onset. Note that in this and following panels, negative is plotted down so that later power traces appear facing upward. *B*: the same EEG signal processed with a 35-Hz bandpass filter. After being filtered, the analytic power was estimated (see METHODS), and this estimate is shown by the thick blue line. *C*: power at 35 Hz for every no-stop trial in the example session. Each horizontal line of color shows a single trial centered on the saccade onset. Warmer colors indicate more power. Note the faint band adjacent to the saccade onset indicating that the 35-Hz bandpass filter was somewhat successful in isolating SP-related activation. *D*: this result is further demonstrated by collapsing across all trials and creating an ERP from the power traces at 35 Hz. A "signal" and "noise" time period was chosen based on SP peak time measured from unfiltered session ERPs. The time period highlighted in white was the signal time period, and the time period in gray was the noise time period for *monkey F*. Average power in both time periods was recorded and used to calculate signal-to-noise ratios (S:N). *E*: the signal-to-noise ratio for each bandpass frequency was calculated for each session. These traces show the average signal-to-noise ratio separately for *monkey F* (blue) and *monkey Y* (green) ± SE. The highest signal-to-noise ratio was found at a bandpass frequency of 95 Hz for *monkey F* (*F*) and 35 Hz for *monkey Y* (*G*).

Since power was baseline corrected to the interval 150–50 ms before target onset, power measurements collected at each SSD could be subjected to *t*-tests, allowing us to test the null hypothesis that canceled trials do not show SP activation in the absence of overt eye movements. The results of this analysis are shown in Fig. 7. Each observation represents the average power for one SSD measured during the period of time when saccades were likely. No-stop trials (Fig. 7, *left*) showed an increase in power above baseline when saccades were produced (mean = 0.26 μV). This increase was statistically significant ($P < 0.001$, df = 167) and demonstrates that there was a reliable increase in SP activation associated with saccades. In contrast, canceled trials (Fig. 7, *right*) showed slightly decreased power during the period of time when saccades were likely to occur (mean = −0.11 μV). Although this effect was small, it was statistically significant ($P < 0.001$, df = 167), suggesting a small but reliable decrease in SP activation during periods when saccades were canceled. Thus, no partial EMG activation was present when monkeys cancelled eye movements in the saccade countermanding task.

DISCUSSION

We have provided evidence indicating that partial muscle activation does not occur in the primate ocular motor system when monkeys inhibit saccades in a countermanding task. Our conclusion is supported by the following observations. First, when canceled ERPs are aligned on a virtual saccade event to create saccade-aligned ERPs, no evidence of EMG activation in the form of a SP can be observed around the time of saccade initiation. Second, when the SP activation is isolated from the surrounding EEG using bandpass filters, no-stop trials show EMG power that is significantly elevated above baseline while saccades are being made. Canceled trials, on the other hand, do not show EMG power that is elevated above baseline. Instead, trials in which saccades were deemed canceled display slightly reduced EMG activation as measured by the SP. This is strong evidence against partial motor activation in the ocular motor system on canceled saccade trials.

The saccadic countermanding paradigm is a versatile tool that has led to many key findings over the last two decades. Human psychophysical experiments using the saccadic stop signal task have helped elucidate the nature of conjugate gaze shifts (Corneil and Elsley 2005), differences between predictive and reactive stimulus tracking (Joiner et al. 2007), the relative contributions of reflexive foveal stimulation to stopping (Cabel et al. 2000), and the influence of stimuli timing and salience on saccade inhibition (Morein-Zamir and Kingstone 2006; Stevenson et al. 2009). Physiological recordings from monkeys carrying out the stop signal task have helped uncover cortical (Hanes et al. 1998; Brown et al. 2008; Ray et al. 2009; Stuphorn et al. 2009; Scangos and Stuphorn 2010) and subcortical (Pare' and Hanes 2003) mechanisms of saccade generation. The task is useful for investigating performance monitoring in both human (Curtis et al. 2005; Endrass et al. 2005)

Downloaded from jn.physiology.org on December 9, 2011

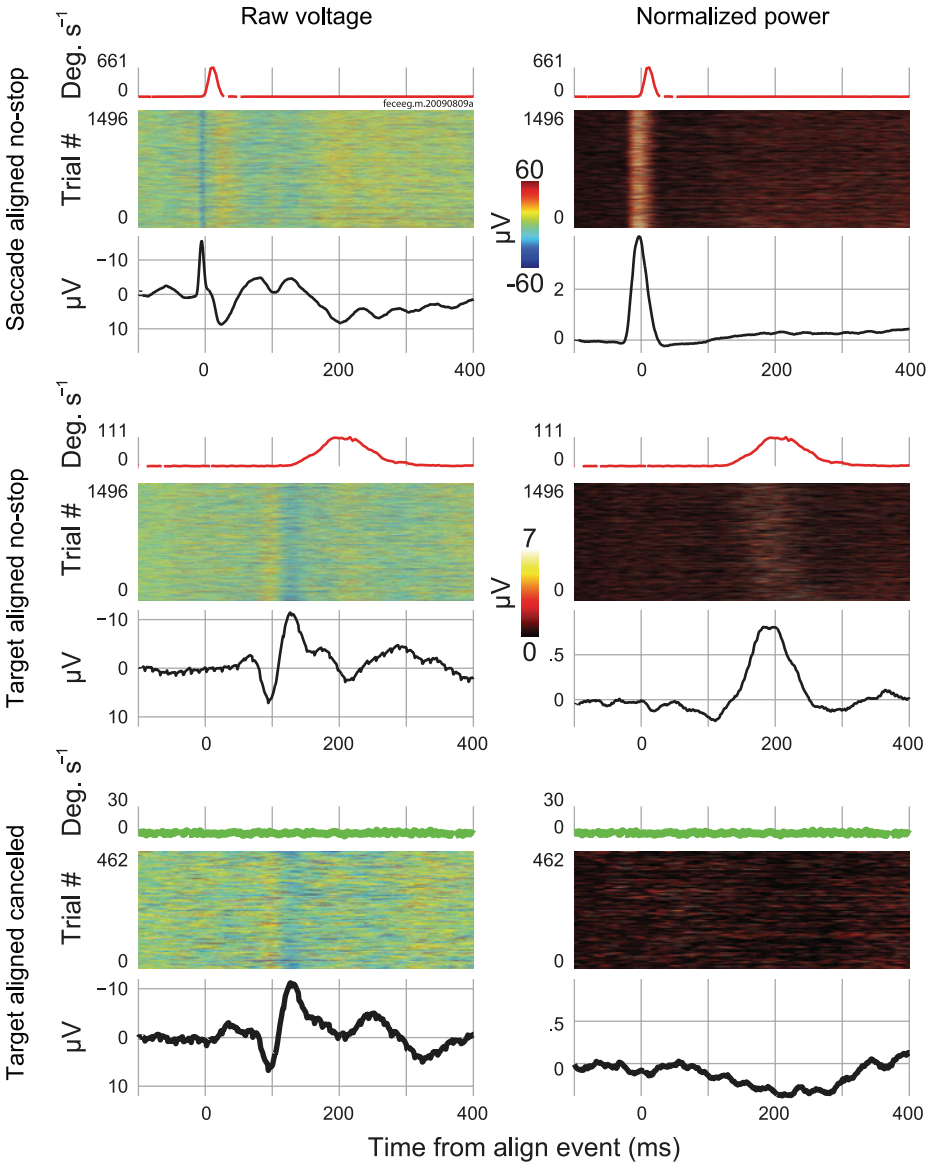

Fig. 6. Filtering EEG makes it possible to observe the SP independent of surrounding EEG, but no SP was observed on canceled trials. Traces at the *top* show ERVs to display saccade timing (conventions as in Fig. 4). Heat maps show individual trials (conventions as in Fig. 5). Black lines show ERPs collapsed across trials. Thin lines show no-stop trial ERPs, and thick lines show canceled trial ERPs. The *left* column displays raw voltage. At the *top*, data are presented from no-stop trials aligned to the saccade onset. The ERV appears as a narrow component beginning at the saccade onset. The heat maps display negative bands of activation at the saccade onset corresponding to the SP. Collapsing across the data in the ERP makes the SP readily apparent in both the raw and filtered data. At the *middle*, data are presented from no-stop trials aligned to the target onset. The ERV reflects this change. Saccades were smeared around 200 ms centered roughly at 210 ms after the target onset. Because of this smearing, it was no longer possible to discern negative activation associated with the SP in the raw heat map. This activation should be apparent centered around 200 ms after the target onset. SP activation was also smeared in the raw ERP, rendering it invisible. However, in the filtered data, SP activation was clear around 200 ms in both the heat map and ERP. At the *bottom*, data are presented from canceled trials aligned to the target onset. The ERV never approached 30°/s (criteria for saccade initiation). No SPs were apparent in the raw heat map data or in the raw ERP. However, it is impossible to tell if no SPs exist, because they were also unobservable in the raw no-stop data plotted above due to overlapping components and smear. The filtered data at *right* allowed for an examination of SP activation. No SP activation was observed in the time around the saccade initiation. If anything, a small depression in high-frequency SP activation was all that could be observed.

and animal (Stuphorn et al. 2000; Ito et al. 2003; Stuphorn and Schall 2006; Emeric et al. 2008, 2010) subjects. In addition, the saccadic countermanding task has given rise to a strong computational modeling literature leading to breakthroughs in understanding neural saccade production and regulation (Hanes and Schall 1996; Asrress and Carpenter 2001; Boucher et al. 2007; Lo et al. 2009; Wong-Lin et al. 2010). Finally, the saccadic stop signal task has had broad clinical significance, providing insights on the action of several popular anesthetic agents (Khan et al. 1999; Nouraei et al. 2003), as well as the core dysfunctions underlying disorders such as mild traumatic brain injury (DeHaan et al. 2007), Parkinson's disease (Joti et al. 2007), and attention-deficit hyperactivity disorder (Armstrong and Munoz 2003; Hanisch et al. 2006). Given the wide experimental significance of the saccadic stop signal paradigm, the observation of partial muscle activation on canceled saccade trials would have provided important theoretical leverage to the study of behavioral inhibition.

Several groups have found partial motor activation on canceled trials during the manual response version of the countermanding task. Partial motor activation on canceled trials has been taken as evidence against a ballistic phase of motor execution (De Jong et al. 1990; McGarry and Franks 1997; McGarry et al. 2000). Partial motor activation has also been used to study the unity or diversity of stopping under different circumstances (De Jong et al. 1990; van Boxtel et al. 2001). In addition, partial motor activation on canceled trials has been compared with full motor activation on no-stop trials, used as a proxy measure for SSRT, and compared with neural data to assess the relative contribution of supplementary motor neurons to movement initiation (Scangos and Stuphorn 2010). Clearly, partial motor activation on canceled trials is a useful measurement for characterizing countermanding behavior. In contrast to manual response countermanding, partial extraocular muscle activation appears to be absent on canceled trials in the saccade countermanding task.

Lack of partial extraocular muscle activation on canceled trials is not surprising given our current understanding of the saccadic system. The saccadic system and spinal motor system differ in several important ways. Unlike manual responses and

Downloaded from jn.physiology.org on December 9, 2011

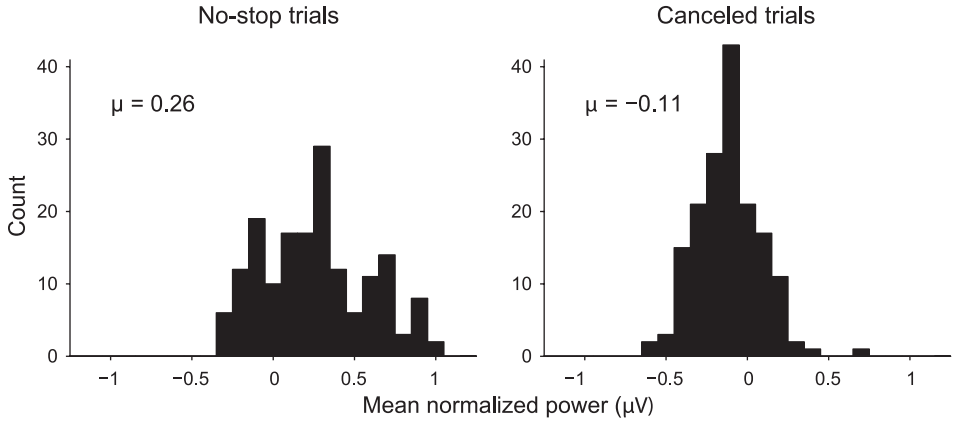

Fig. 7. No-stop trial EEGs display significantly increased SP activation during periods when saccades are produced, but canceled trial EEGs show no increase in SP activation. After trials had been latency matched and EEG data filtered (see Fig. 6), the average power during a discreet time window was measured on a trial-by-trial basis. For the time window, we chose the period between the 25th and 75th RT percentiles. Since no-stop trials were latency matched to canceled trials, this is the period of time during which SP activation was most likely to occur in both trial types. Power averages were collected from this time window at each SSD. Each SSD from each recorded session yielded a single observation for each trial type. The histograms show the results of this analysis. The observations are gathered in 0.1-μV bins for display purposes. Grand average power is reported for each trial type above the appropriate histogram. Note that the sign of these averages is negative for canceled trials. Both distributions deviated significantly from zero (Students t-test, $P < 0.001$, degrees of freedom = 167).

smooth pursuit eye movements, saccade initiation is, in many ways, ballistic (for reviews, see Sparks 2002; Scudder et al. 2002). Kornylo and colleagues (2003) found that pursuit eye movements could be canceled more quickly than saccadic eye movements and concluded that saccade production includes a final ballistic stage that is not observed during pursuit.

One possible criticism of this work concerns the linking proposition identifying the SP with the extraocular EMG. Since its first observation and characterization as the external rectus muscle potential (Blinn 1955), the SP has been almost uniformly appreciated as myogenic in nature (Picton et al. 2000; but see also Kurtzberg and Vaughan 1982; Balaban and Weinstein 1985; Riemslag et al. 1988). This conclusion is supported by the following seven observations. First, the corneoretinal potential cannot contribute to the SP since the SP can still be recorded in total darkness (Riggs et al. 1974; Moster and Goldberg 1990) and observed in patients with ocular prosthesis and intact extraocular musculature (Thickbroom and Mastaglia 1985). Second, the SP is not considered to be cortical in origin, since it has been obtained with normal topography after complete hemispherectomy (Thickbroom and Mastaglia 1985). Third, the SP is attenuated or absent in patients with lateral rectus palsy or patients in whom the intraorbital musculature has been surgically removed (Thickbroom and Mastaglia 1985). Fourth, the amplitude of the SP remains constant, but its scalp distribution changes predictably with saccades made in different directions (Thickbroom and Mastaglia 1985; Moster and Goldberg 1990; Keren et al. 2010). Fifth, both its scalp distribution (Moster and Goldberg 1990; Lins et al. 1993a; Keren et al. 2010; Sander et al. 2010) and dipole source modeling (Thickbroom and Mastaglia 1985; Lins et al. 1993b) suggest that the SP is maximal around the eyes. Sixth, there is a close and consistent timing correlation between the peak of the SP and saccade onset (Thickbroom and Mastaglia 1985; Keren et al. 2010). Finally, the amplitude of the SP shows a positive correlation with saccade amplitude (Keren et al. 2010). Thus, using the strong inference method advocated by Platt (1964), an extensive body of evidence has demonstrated that the SP should be viewed as an extraocular EMG. It is a natural step, then, to search for the presence of extraocular EMG activation using SPs recorded in the stop signal task.

Another possible criticism concerns the resolution of our EMG measurement. One may argue that our proxy measure of extraocular EMG was not sensitive enough to detect small muscle activations. If so, partial muscle activation may have been present on some canceled trials that was unobservable as single trial SP. Using a wide bandpass filter, Keren et al. (2010) were able to reliably isolate single SPs from the raw EEG. They then used signal detection theory to quantify the accuracy with which single SPs predict saccades. These researchers found that they could detect >80% of saccades 0.5–1° in amplitude with close to zero false alarms, and they could detect saccades of 0.02–0.2° in amplitude above chance level. They concluded that single SPs might serve as more reliable saccade indicators than the traditional method of detecting corneoretinal dipole shifts in EEG recordings.

We refined the technique presented by Keren et al. (2010) by adopting a frequency optimization procedure that ensured small SPs would be highly detectable. The average power traces that we were able to construct for no-stop trials containing 10° saccades suggest that we would have been able to detect SPs associated with very small amplitude movements (see Figs. 5 and 6). Still, the fact remains that canceled trials may be associated with subthreshold EMG activation that is too small to detect with surface electrodes. To test this hypothesis further, recordings would be needed from microelectrodes inserted into the motor nuclei themselves.

It is noteworthy that we did not simply observe a lack of extraocular EMG on canceled saccade trials. Instead, we report a small but significant decrease in EMG activity when eye movements were withheld. Before baselining, a tonic increase in EMG was observed in the period of time around task-related saccades. (Fig. 5, *F* and *G*) We speculate that this tonic resting EMG activity was produced by microsaccades that occurred throughout our recordings (Yuval-Greenberg et al. 2008). On canceled trials, we observed a significant decrease in tonic EMG activity during periods when saccades were likely (Fig.

Downloaded from jn.physiology.org on December 9, 2011

6, *bottom right*). Following this logic, we suggest that fewer microsaccades are probably made while eye movements are suppressed during canceled trials. This would be an interesting finding, useful for further characterizing the function of fixation cells during the countermanding task. Unfortunately, the spatial resolution of our current eye tracking data set does not allow us to test this hypothesis directly. Future work should measure the presence or absence of microsaccades during periods when task-related saccades are canceled in the countermanding task.

In summary, we isolated EMG activation associated with eye movements from the EEGs of monkeys performing a saccade countermanding task. We found that eye movements were reliably accompanied by EMG activation on noncanceled trials, but no subthreshold EMG activation was detectable on successfully canceled trials. This finding demonstrates the ballistic nature of saccade initiation and highlights a basic difference between the spinal motor system and the saccadic ocular motor system.

ACKNOWLEDGMENTS

The authors thank C. Segovis for invaluable contributions throughout this work. M. Feurtado, M. Young, and P. Weigand helped with animal care. K. Thakkar and P. Bissett provided useful comments on the manuscript.

GRANTS

This work was supported by National Institutes of Health Grants R01-MH-55806, R01-EY-019882, P30-EY-08126, and P30-HD-015052 and by Robin and Richard Patton through the E. Bronson Ingram Chair in Neuroscience.

DISCLOSURES

No conflicts of interest, financial or otherwise, are declared by the author(s).

REFERENCES

Anderson SR, Porrill J, Sklavos S, Gandhi NJ, Sparks DL, Dean P. Dynamics of primate oculomotor plant revealed by effects of abducens microstimulation. *J Neurophysiol* 101: 2907–2923, 2009.

Armstrong IT, Munoz DP. Inhibitory control of eye movements during oculomotor countermanding in adults with attention-deficit hyperactivity disorder. *Exp Brain Res* 152: 444–452, 2003.

Asrress KN, Carpenter RH. Saccadic countermanding: a comparison of central and peripheral stop signals. *Vision Res* 41: 2645–2651, 2001.

Balaban CD, Weinstein JM. The human pre-saccadic spike potential–influences of a visual target, saccade direction, electrode laterality and instructions to perform saccades. *Brain Res* 347: 49–57, 1985.

Band GPH, van der Molen MW, Logan GD. Horse-race model simulations of the stop-signal procedure. *Acta Psychol* 112: 105–142, 2003.

Blinn KA. Focal anterior temporal spikes from external rectus muscles. *Electroencephalogr Clin Neurophysiol* 7: 299–302, 1955.

Boucher L, Palmeri TJ, Logan GD, Schall JD. Inhibitory control in mind and brain: an interactive race model of countermanding Saccades. *Psychol Rev* 114: 376–397, 2007.

Boucher L, Stuphorn V, Logan GD, Schall JD, Palmeri TJ. Stopping eye and hand movements: are the processes independent? *Percept Psychophys* 69: 785–801, 2007.

Brown JW, Hanes DP, Schall JD, Stuphorn V. Relation of frontal eye field activity to saccade initiation during a countermanding task. *Exp Brain Res* 190: 135–151, 2008.

Cabel DW, Armstrong IT, Reingold E, Munoz DP. Control of saccade initiation in a countermanding task using visual and auditory stop signals. *Exp Brain Res* 133: 431–441, 2000.

Collewijn H, Kowler E. The significance of microsaccades for vision and oculomotor control. *J Vision* 8: 2008.

Colonius H. A note on the stop-signal paradigm, or how to observe the unobservable. *Psychol Rev* 97: 309–312, 1990.

Corneil BD, Elsley JK. Countermanding eye-head gaze shifts in humans: marching orders are delivered to the head first. *J Neurophysiol* 94: 883–895, 2005.

Curtis CE, Cole MW, Rao VY, D'Esposito M. Canceling planned action: an fMRI study of countermanding saccades. *Cereb Cortex* 15: 1281–1289, 2005.

De Jong R, Coles MG, Logan GD, Gratton G. In search of the point of no return-the control of response processes. *J Exp Psychol Hum Percept Perform* 16: 164–182, 1990.

DeHaan A, Halterman C, Langan J, Drew AS, Osternig LR, Chou LS, van Donkelaar P. Cancelling planned actions following mild traumatic brain injury. *Neuropsychologia* 45: 406–411, 2007.

Emeric EE, Brown JW, Boucher L, Carpenter RH, Hanes DP, Harris R, Logan GD, Mashru RN, Pare M, Pouget P, Stuphorn V, Taylor TL, Schall JD. Influence of history on saccade countermanding performance in humans and macaque monkeys. *Vision Res* 47: 35–49, 2007.

Emeric EE, Brown JW, Leslie M, Pouget P, Stuphorn V, Schall JD. Performance monitoring local field potentials in the medial frontal cortex of primates: anterior cingulate cortex. *J Neurophysiol* 99: 759–772, 2008.

Emeric EE, Leslie M, Pouget P, Schall JD. Performance monitoring local field potentials in the medial frontal cortex of primates: supplementary eye field. *J Neurophysiol* 104: 1523–1537, 2010.

Endrass T, Cosima F, Norbert K. Error awareness in a saccade countermanding task. *J Psychophysiol* 19: 275–280, 2005.

Evdokimidis I, Liakopoulos D, Papageorgiou C. Cortical potentials preceding centrifugal and centripetal self-paced horizontal saccades. *Electroencephalogr Clin Neurophysiol* 79: 503–505, 1991.

Everling S, Krappmann P, Flohr H. Cortical potentials preceding pro- and antisaccades in man. *Electroencephalogr Clin Neurophysiol* 102: 356–362, 1997.

Fuchs AF, Luschei ES. Firing patterns of abducens neurons of alert monkeys in relationship to horizontal eye movement. *J Neurophysiol* 33: 382–392, 1970.

Godlove DC, Emeric EE, Boucher L, Schall JD. Express saccade production in a stop signal task. Program No. 71.6 2009 Neuroscience Meeting Planner. Chicago, IL: Soc for Neuroscience, 2009. Online. *Soc Neurosci Abstract*: 2009.

Hanes DP, Carpenter RH. Countermanding saccades in humans. *Vision Res* 39: 2777–2791, 1999.

Hanes DP, Patterson WF, Schall JD. Role of frontal eye fields in countermanding saccades: visual, movement, and fixation activity. *J Neurophysiol* 79: 817–834, 1998.

Hanes DP, Schall JD. Countermanding saccades in macaque. *Vis Neurosci* 12: 929–937, 1995.

Hanes DP, Schall JD. Neural control of voluntary movement initiation. *Science* 274: 427–430, 1996.

Hanisch C, Radach R, Holtkamp K, Herpertz-Dahlmann B, Konrad K. Oculomotor inhibition in children with and without attention-deficit hyperactivity disorder (ADHD). *J Neural Transm* 113: 671–684, 2006.

Hikosaka O, Igusa Y, Nakao S, Shimazu H. Direct inhibitory synaptic linkage of pontomedullary reticular burst neurons with abducens motoneurons in cat. *Exp Brain Res* 33: 337–352, 1978.

Ito S, Stuphorn V, Brown JW, Schall JD. Performance monitoring by the anterior cingulate cortex during saccade countermanding. *Science* 302: 120–122, 2003.

Joiner WM, Lee JE, Shelhamer M. Behavioral analysis of predictive saccade tracking as studied by countermanding. *Exp Brain Res* 181: 307–320, 2007.

Joti P, Kulashekhar S, Behari M, Murthy A. Impaired inhibitory oculomotor control in patients with Parkinson's disease. *Exp Brain Res* 177: 447–457, 2007.

Keren AS, Yuval-Greenberg S, Deouell LY. Saccadic spike potentials in gamma-band EEG: characterization, detection and suppression. *Neuroimage* 49: 2248–2263, 2010.

Khan O, Taylor SJ, Jones JG, Swart M, Hanes DP, Carpenter RH. Effects of low-dose isoflurane on saccadic eye movement generation. *Anaesthesia* 54: 142–145, 1999.

Kornylo K, Dill N, Saenz M, Krauzlis RJ. Canceling of pursuit and saccadic eye movements in humans and monkeys. *J Neurophysiol* 89: 2984–2999, 2003.

Kurtzberg D, Vaughan HG. Topographic analysis of human cortical potentials preceding self-initiated and visually triggered saccades. *Brain Res* 243: 1–9, 1982.

Lins OG, Picton TW, Berg P, Scherg M. Ocular artifacts in EEG and event-related potentials. I: scalp topography. *Brain Topogr* 6: 51–63, 1993a.

Downloaded from jn.physiology.org on December 9, 2011

Lins OG, Picton TW, Berg P, Scherg M. Ocular artifacts in recording EEGs and event-related potentials. II: source dipoles and source components. *Brain Topogr* 6: 65–78, 1993b.

Lo CC, Boucher L, Pare M, Schall JD, Wang XJ. Proactive inhibitory control and attractor dynamics in countermanding action: a spiking neural circuit model. *J Neurosci* 29: 9059–9071, 2009.

Logan GD. On the ability to inhibit thought and action: a users' guide to the stop signal paradigm. In: *Inhibitory Processes in Attention, Memory, and Language*, edited by Dagenback D, Carr TH. San Diego, CA: Academic, 1994, p. 189–239.

Logan GD, Cowan WB. On the ability to inhibit thought and action–a theory of an act of control. *Psychol Rev* 91: 295–327, 1984.

Logan GD, Irwin DE. Don't look! Don't touch! Inhibitory control of eye and hand movements. *Psychon Bull Rev* 7: 107–112, 2000.

McGarry T, Franks IM. A horse race between independent processes: evidence for a phantom point of no return in the preparation of a speeded motor response. *J Exp Psychol Hum Percept Perform* 23: 1533–1542, 1997.

McGarry T, Inglis JT, Franks IM. Against a final ballistic process in the control of voluntary action: evidence using the Hoffmann reflex. *Motor Control* 4: 469–485, 2000.

Morein-Zamir S, Kingstone A. Fixation offset and stop signal intensity effects on saccadic countermanding: a crossmodal investigation. *Exp Brain Res* 175: 453–462, 2006.

Moster ML, Goldberg G. Topography of scalp potentials preceding self-initiated saccades. *Neurology* 40: 644–648, 1990.

Nouraei SAR, de Pennington N, Jones JG, Carpenter RH. Dose-related effect of sevoflurane sedation on higher control of eye movements and decision making. *Br J Anaesth* 91: 175–183, 2003.

Nunez PL, Srinivasan R. *Electric Fields of the Brain: the Neurophysics of EEG*. Oxford: Oxford Univ. Press, 2006.

Pare' M, Hanes DP. Controlled movement processing: superior colliculus activity associated with countermanded saccades. *J Neurosci* 23: 6480–6489, 2003.

Picton TW, van Roon P, Armilio ML, Berg P, Ille N, Scherg M. Blinks, saccades, extraocular muscles and visual evoked potentials (reply to Verleger). *J Psychophysiol* 14: 210–217, 2000.

Platt JR. Strong inference. *Science* 146: 347–353, 1964.

Porter JD, Andrade FH, Baker RS. The extraocular muscles. In: *Adler's Physiology of the Eye*, edited by Kaufman PL, Alm A. St. Louis, MO: Mosby, 2003, p. 787–817.

Quaia C, Optican LM. Three-dimensional rotations of the eye. In: *Adler's Physiology of the Eye*, edited by Kaufman PL, Alm A. St. Louis, MO: Mosby, 2003, p. 818–829.

Quaia C, Ying HS, Optican LM. The viscoelastic properties of passive eye muscle in primates. III: force elicited by natural elongations. *PLoS One* 5: A236–A254, 2009.

Ray S, Pouget P, Schall JD. Functional distinction between visuomovement and movement neurons in macaque frontal eye field during saccade countermanding. *J Neurophysiol* 102: 3091–3100, 2009.

Riemslag FC, Vanderheijde GL, Vandongen MM, Ottenhoff F. On the origin of the presaccadic spike potential. *Electroencephalogr Clin Neurophysiol* 70: 281–287, 1988.

Riggs LA, Merton PA, Morton HB. Suppression of visual phosphenes during saccadic eye-movements. *Vision Res* 14: 997–1011, 1974.

Robinson DA. The mechanics of human saccadic eye movement. *J Physiol* 174: 245–264, 1964.

Robinson DA. Oculomotor unit behavior in monkey. *J Neurophysiol* 33: 393–403, 1970.

Sander V, Soper B, Everling S. Nonhuman primate event-related potentials associated with pro- and anti-saccades. *Neuroimage* 49: 1650–1658, 2010.

Scangos KW, Stuphorn V. Medial frontal cortex motivates but does not control movement initiation in the countermanding task. *J Neurosci* 30: 1968–1982, 2010.

Scudder CA, Kaneko CR, Fuchs AF. The brainstem burst generator for saccadic eye movements–a modern synthesis. *Exp Brain Res* 142: 439–462, 2002.

Sklavos S, Porrill J, Kaneko CR, Dean P. Evidence for wide range of time scales in oculomotor plant dynamics: implications for models of eye-movement control. *Vision Res* 45: 1525–1542, 2005.

Sparks DL. The brainstem control of saccadic eye movements. *Nat Rev Neurosci* 3: 952–964, 2002.

Stevenson SA, Elsley JK, Corneil BD. A "gap effect" on stop signal reaction times in a human saccadic countermanding task. *J Neurophysiol* 101: 580–590, 2009.

Stuphorn V, Brown JW, Schall JD. Role of supplementary eye field in saccade initiation: executive, not direct, control. *J Neurophysiol* 103: 801–16, 2009.

Stuphorn V, Schall JD. Executive control of countermanding saccades by the supplementary eye field. *Nat Neurosci* 9: 925–931, 2006.

Stuphorn V, Taylor TL, Schall JD. Performance monitoring by the supplementary eye field. *Nature* 408: 857–860, 2000.

Thickbroom GW, Mastaglia FL. Presaccadic spike potential–investigation of topography and source. *Brain Res* 339: 271–280, 1985.

van Boxtel GJ, van der Molen MW, Jennings JR, Brunia CH. A psychophysiological analysis of inhibitory motor control in the stop-signal paradigm. *Biol Psychol* 58: 229–262, 2001.

Verbruggen F, Logan GD. Response inhibition in the stop-signal paradigm. *Trends Cogn Sci* 12: 418–424, 2008.

Walton MM, Gandhi NJ. Behavioral evaluation of movement cancellation. *J Neurophysiol* 96: 2011–2024, 2006.

Wong-Lin K, Eckhoff P, Holmes P, Cohen JD. Optimal performance in a countermanding saccade task. *Brain Res* 1318: 178–187, 2010.

Woodman GF, Kang MS, Rossi AF, Schall JD. Nonhuman primate event-related potentials indexing covert shifts of attention. *Proc Natl Acad Sci USA* 104: 15111–15116, 2007.

Yuval-Greenberg S, Tomer O, Keren AS, Nelken I, Deouell LY. Transient induced gamma-band response in EEG as a manifestation of miniature saccades. *Neuron* 58: 429–441, 2008.

Downloaded from jn.physiology.org on December 9, 2011